THE EUROPEAN PHYSICAL JOURNAL C

Regular Article - Experimental Physics

Performance of thin-RPC detectors for high rate applications with eco-friendly gas mixtures

RPC ECOGas@GIF++ Collaboration

M. Abbrescia[1,2], G. Aielli[4,5], R. Aly[1,6], M. C. Arena[7], M. Barroso Ferreira Filho[8], L. Benussi[9], S. Bianco[9], F. Bordon[10], D. Boscherini[11], A. Bruni[11], S. Buontempo[12], M. Busato[10], P. Camarri[4,5], R. Cardarelli[4], L. Congedo[1], M. De Serio[1,2], A. Di Ciaccio[4,5], L. Di Stante[4,5], P. Dupieux[13], J. Eysermans[14], A. Ferretti[15,16], G. Galati[2,1,a], M. Gagliardi[15,16], R. Guida[10], G. Iaselli[1,3], B. Joly[13], K. S. Lee[17], B. Liberti[4], B. Mandelli[10], S. P. Manen[13], A. Pastore[1,b], E. Pastori[4], D. Piccolo[9], L. Pizzimento[4], A. Polini[11], G. Proto[4,5], G. Pugliese[1,3], L. Quaglia[15], D. Ramos[1,3], G. Rigoletti[10], A. Rocchi[4], M. Romano[11], A. Samalan[19], P. Salvini[20], R. Santonico[4,5], G. Saviano[21], M. Sessa[4], S. Simone[1,2], L. Terlizzi[15,16], M. Tytgat[19,22], E. Vercellin[15,16], M. Verzeroli[10,23], N. Zaganidis[18]

1 INFN Sezione di Bari, Via E. Orabona 4, 70125 Bari, Italy
2 Dipartimento Interateneo di Fisica, Università of Bari, Via Amendola 173, 70125 Bari, Italy
3 Dipartimento Interateneo di Fisica, Politecnico di Bari, Via Amendola 173, 70125 Bari, Italy
4 INFN Sezione di Roma Tor Vergata, Via della Ricerca Scientifica 1, 00133 Rome, Italy
5 Dipartimento di Fisica, Università degli studi di Roma Tor Vergata, Via della Ricerca Scientifica 1, 00133 Rome, Italy
6 Helwan University, Helwan Sharkeya, Helwan, Cairo Governorate 4037120, Egypt
7 Università degli studi di Pavia, Corso Strada Nuova 65, 27100 Pavia, Italy
8 Universidade do Estado do Rio de Janeiro, R. Sao Francisco Xavier, 524-Maracaná, Rio de Janeiro, RJ 20550-013, Brazil
9 INFN-Laboratori Nazionali di Frascati, Via Enrico Fermi 54, Frascati, 00044 Rome, Italy
10 CERN, Espl. des Particules 1, 1211 Meyrin, Switzerland
11 INFN Sezione di Bologna, Viale C. Berti Pichat 4/2, 40127 Bologna, Italy
12 INFN Sezione di Napoli, Complesso Universitario di Monte S. Angelo ed. 6, Via Cintia, 80126 Naples, Italy
13 Clermont Université, Université Blaise Pascal, CNRS/IN2P3, Laboratoire de Physique Corpusculaire, BP 10448, 63000 Clermont-Ferrand, France
14 Massachusetts Institute of Technology, 77 Massachusetts Ave, Cambridge, MA 02139, USA
15 INFN Sezione di Torino, Via P. Giuria 1, 10126 Turin, Italy
16 Dipartimento di Fisica, Università degli studi di Torino, Via P. Giuria 1, 10126 Turin, Italy
17 Department of Physics, Korea University, Seoul, Korea
18 Dept. de Fisica y Matematicas, Universidad Iberoamericana, 01210 Mexico City, Mexico
19 Department of Physics and Astronomy, Ghent University, Proeftuinstraat 86, 9000 Ghent, Belgium
20 INFN Sezione di Pavia, Via A. Bassi 6, 27100 Pavia, Italy
21 Dipartimento di Ingegneria Chimica Materiali Ambiente, Università di Roma Sapienza, Piazzale Aldo Moro 5, 00185 Rome, Italy
22 Department of Physics, Vrije Universiteit Brussel (VUB-ELEM), Pleinlaan 2, 1050 Brussels, Belgium
23 Université Claude Bernard Lyon I, 43 Bd du 11 Novembre 1918, 69100 Villeurbanne, France

Abstract In the last few years, an intense R&D activity on particle detectors for future HEP applications has been carried on with the aim of developing new techniques as well as studying the performance of already existing detectors when operated in a high rate environment. As for Resistive Plate Chamber detectors, the main challenges to face are the improvement of their detection capabilities and longevity at very high-rates, and the search for new eco-friendly gasmixtures free from greenhouse components. Results obtained in the framework of the RPC ECO-Gas@GIF++ Collaboration on a thin-Resistive Plate Chamber exposed at the CERN Gamma Irradiation Facility and operated with eco-friendly gas mixtures based on Tetrafluoropropene and Carbon dioxide will be discussed in this paper.

1 Introduction

Resistive Plate Chamber (RPC) detectors have been playing a significant role in particle physics experiments since

a e-mail: giuliana.galati@ba.infn.it (corresponding author)

b e-mail: alessandra.pastore@ba.infn.it (corresponding author)

Springer

decades. Currently, RPCs with a typical 2 mm-thick gas gap show a rate capability of about 1 kHz/cm^2 when operated in avalanche mode [1] with a gas mixture made of 95.2% $C_2H_2F_4$, 4.5% i-C_4H_{10} and 0.3% SF_6, hereafter called *standard*.

Their nanosecond time resolution and few millimetre spatial resolution make them particularly suitable for triggering and tracking purposes with a typical detection efficiency for charged particles of about 98%.

An intense R&D activity is ongoing in view of future applications at colliders with the aim of improving the RPC detection rates up to tens of kHz/cm^2 [2] in combination with new eco-friendly gas mixtures, free from greenhouse (GHG) components. Indeed, the European Commission "F-gas regulation" 517/2014 [3] forces to a severe reduction of GHG emissions by 2030 and drastically limits the amount of F-gases that can be sold. The RPC standard gas mixture mainly contains $C_2H_2F_4$ and SF_6, which have a high Global Warming Potential (GWP),[1] about 1430 and 22,800 respectively [3]. On a short-term time scale, a solution could be the recovery and reuse of the exhaust gas mixture [4–7]; in the long-term other strategies should also be implemented, since the availability and prices of fluorinated gas are not predictable.

Test-campaigns to study the performance of RPC detectors when operated in avalanche mode at high rate in combination with new eco-friendly gas mixtures are being carried on at the Gamma Irradiation Facility (GIF++) [8] at CERN, in the framework of the RPC ECOGas@GIF++ Collaboration. In the present paper, results obtained in different background conditions with a thin RPC chamber exposed to the 662 keV photon source with adjustable intensity are presented.

2 RPC detectors for future applications

In HEP, RPC detectors [9] with 2 mm gas gaps and 2 mm electrodes thickness have been usually operated at a voltage (*working point*, WP) of about 10 kV when flushed with the aforementioned standard gas mixture.

The higher particle rate foreseen in future applications will lead to an increase of the WP for such a detector layout. Indeed, when the detector is exposed to a particle rate per unit surface Φ, the voltage applied to the gas gap HV_{gas} is locally reduced by a drop (HV_d) that can be expressed as: $HV_d = 2\,\Phi\rho d\,<Q>$, where d is the thickness of the electrodes, ρ their resistivity, and $<Q>$ the average charge released in the gas from a single ionising particle crossing the gap. In order to keep HV_{gas} constant at higher particle rates,

higher applied voltages HV_{app} are required, since $HV_{gas} = HV_{app} - HV_d$ [10].

Decreasing d, ρ or $<Q>$ would reduce the voltage drop at high rates, avoiding a significant increase in HV_{app} as well as limiting the current-induced ageing of the detector [11–14].

As for GHG emissions, the scientific community is currently investigating possible replacements for $C_2H_2F_4$, the main component of the standard RPC gas mixture.

Among the Hydrofluoroolefyns (HFOs) used for industrial applications, HFO-1234ze ($C_3H_2F_4$, in the following HFO) is of particular interest as $C_2H_2F_4$ substitute since it is neither flammable nor toxic and has a very low GWP, equal to 7 [3]. HFO contains the same amount of fluorine atoms as $C_2H_2F_4$ but one more carbon, resulting in a higher binding energy and a lower first effective Townsend coefficient at a given electric field strength [15]. For these reasons, completely replacing $C_2H_2F_4$ with HFO in RPCs would result in a significant increase of the WP, which should be avoided. The addition of a certain fraction of CO_2 to the gas mixture is being explored as a possible solution. Several mixtures with different fractions of CO_2 and HFO have been tested and first results on the performance obtained with such mixtures can be found in [16–22].

In the following, detailed studies on a RPC with thin gas gap and electrodes, operated with HFO/CO_2-based gas mixtures and exposed at the CERN GIF++ at particle rates up to several kHz/cm^2, will be discussed.

3 Thin-RPC exposure at the CERN Gamma Irradiation Facility

The performance of a single-gap RPC, with gap and High Pressure Laminates (HPL) electrodes[2] each 1.6 mm thick, was studied during dedicated campaigns held in 2021 and 2022 at the CERN GIF++. The RPC active area was (70.6 × 100.6) cm^2.

The thin-RPC was partially instrumented with 32 strips (strip pitch 10.625 mm) both in the horizontal and vertical planes faced on the two gap sides. For signal preamplification and discrimination, the readout strips were connected to Front-End Electronics Rapid Integrated Circuit (FEERIC) ASICs boards, developed for the ALICE Muon Identification System [23]. They provide low voltage differential signals (LVDS) to the Data Acquisition system, a CAEN TDC mod.V1190A.

The detector was exposed to a about 13 TBq ^{137}Cs source, emitting 662 keV gamma rays, in combination with a 100 GeV muon beam from the secondary SPS beam line

---

[1] GWP is defined as the cumulative radiative forcing, here over a 100 years horizon, resulting from the emission of a unit mass of gas related to some reference gas, usually CO_2.

[2] Gap and electrodes were produced by the Korea Detector Laboratory (KODEL). The bulk resistivity of the electrodes is approximately $\rho = 150\ k\Omega/\square$
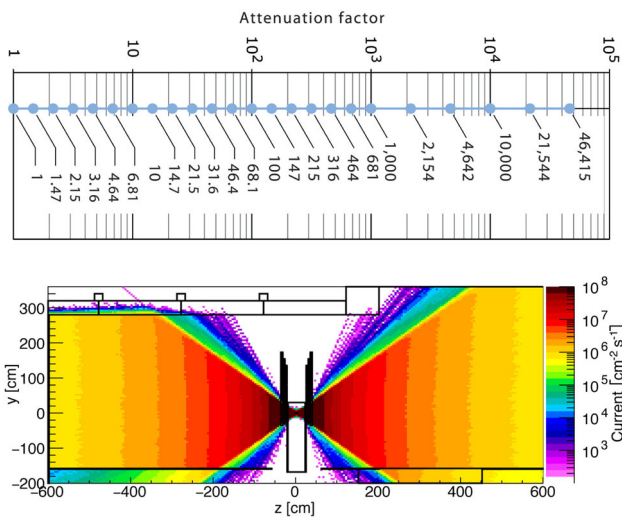
Fig. 1 Top: Each set of movable attenuation filters, with 27 combinations of filters, leads to 24 different attenuation factors between 1 and 46,415. Bottom: Photon density current in the vertical yz plane through the source at $x = 0.65$ m; attenuation filters at factor 1. With angular correction filters, the current of 662 keV photons is made uniform in xy planes [8]
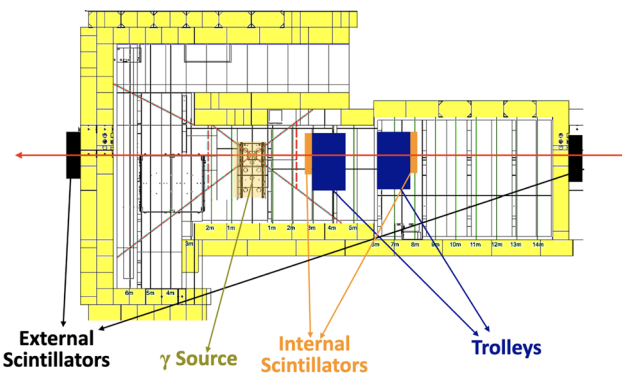

Fig. 2 Layout of the experimental setup at GIF++. The muon beam line is indicated in red

Fig. 3 Typical muon window as defined in the 5 μs trigger time interval

overall trigger area of about 10×10 cm^2 and an average number of triggers per spill equal to about 3000. For each trigger, a time window of 5 μs is open, signals are acquired and finally processed.

Two different HFO-based eco-friendly gas mixtures have been tested and compared with the standard one: the first one (in the following, eco2) is made up by 35% HFO, 60% CO$_2$, 4% iC$_4$H$_{10}$, 1% SF$_6$, while the second one (in the following, eco3) consists of 25% HFO, 69% CO$_2$, 5% iC$_4$H$_{10}$ and 1% SF$_6$.

4 Study of the thin-RPC performance

In the following, the main RPC performances both at 6 m and 3 m from the source are reported in terms of muon identification efficiency, average cluster size, and absorbed current. For each gas mixture, the results are compared at different levels of irradiation, expressed by means of the gamma cluster rate as measured by the detector.

The performances related to the muon signal are evaluated within a window, hereafter referred to as *muon window*, which is defined as the interval of time in which the beam spill occurs. The muon window is estimated by performing a Gaussian fit of the hit time profile acquired by the TDC, as shown in Fig. 3, and its typical value is about 50 ns.

The trend of the relevant variables will be shown as a function of the effective High Voltage (HV$_{eff}$), defined as:

$$HV_{eff} = HV_{app} \frac{p_0 \cdot T}{p \cdot T_0} \qquad (1)$$

where p is the atmospheric pressure and T is the temperature during data-taking, while $p_0 = 990$ hPa and $T_0 = 293.15$ K are average values of temperature and pressure as measured at GIF++.

H4 [24]. A system of lead absorption filters (ABS) can be used to adjust the rate of photons impinging on the detectors, as shown in Fig. 1 top. Further angular correction filters provide uniform irradiation at a fixed distance from the source, as shown in Fig. 1 bottom for the maximum gamma rate available (ABS = 1). The source can also be fully shielded (source off) and tests can be carried on with the muon beam only.

The layout of the experimental setup is shown in Fig. 2. The irradiation tests have been conducted varying both the intensity of the gamma source, ranging from source off up to ABS 1, and the position of the thin-RPC detector, placed respectively 6 m and 3 m far from the source on dedicated trolleys. Signal acquisition has been triggered by the coincidence of four scintillators, two of them placed outside the experimental area while the other two inside, resulting in an
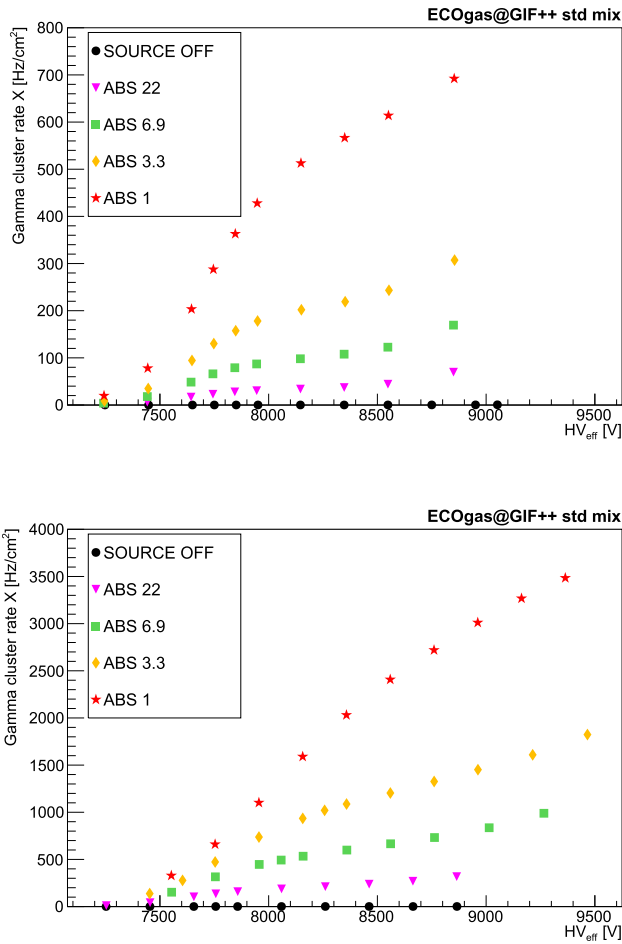
Fig. 4 Gamma cluster rate as a function of HV_{eff} for the thin-RPC operated with standard gas mixture. Results are shown for the vertical strip plane, at 6 m (top) and 3 m (bottom) from the source
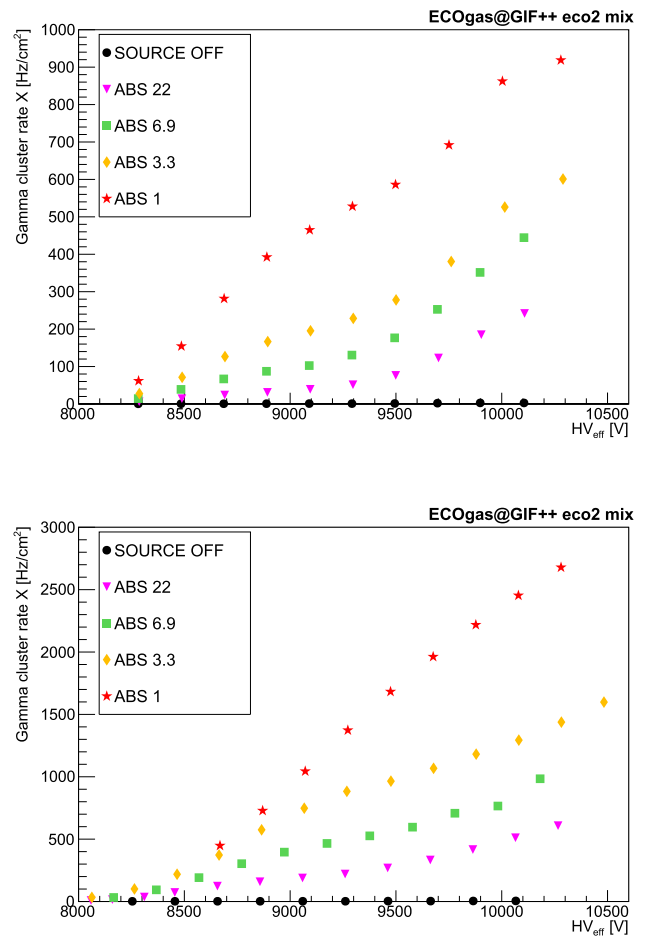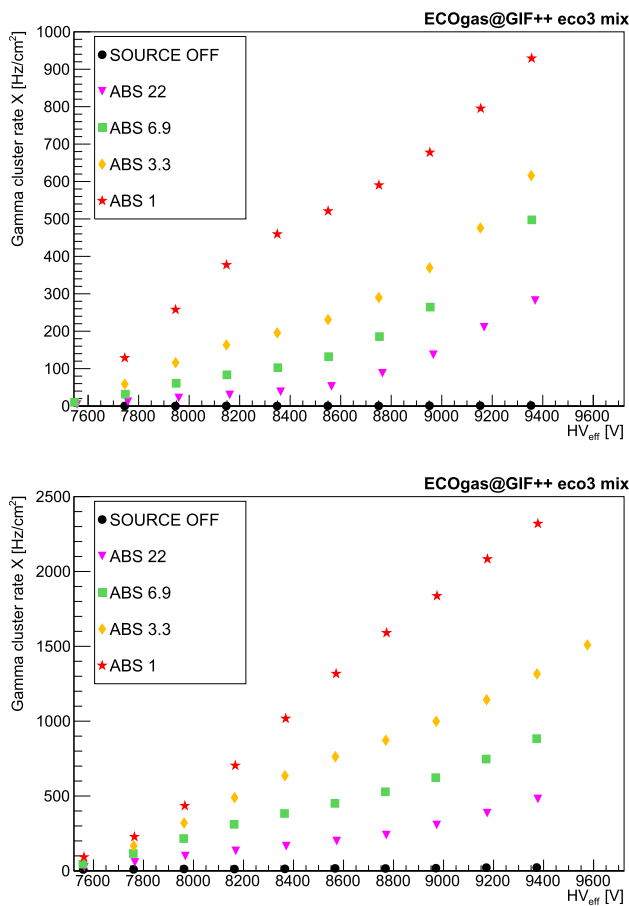

Fig. 5 Gamma cluster rate as a function of HV_{eff} for the thin-RPC operated with eco2 gas mixture. Results are shown for the vertical strip plane, at 6 m (top) and 3 m (bottom) from the source

4.1 Gamma rates

The gamma cluster rate is defined as the total number of detected hits per strips area, divided by the total time interval of the measurement, and normalised to the average cluster size. For both the horizontal and vertical strip planes, it has been evaluated by means of multiple 5µs-long data acquisitions during the interspill interval.

The gamma cluster rate is shown as a function of HV_{eff} in Figs. 4, 5 and 6 for the three gas mixtures. Hereafter, only the distributions relating to the vertical strips will be reported, being representative of the horizontal ones as well.

As expected, an increase of the gamma cluster rate with growing HV_{eff} is observed independently of the gas mixture. The increase is as fast as the irradiation level gets higher, reaching a value of about 1 kHz/cm^2 and about 4 kHz/cm^2 for ABS 1 and full efficiency,[3] when the distance from the source is 6 m and 3 m respectively.

4.2 Efficiency

The 2D muon identification efficiency is evaluated as the number of events with at least one hit inside the muon window, both on the horizontal and vertical strip planes, divided by the total number of triggers.

The efficiency as a function of HV_{eff} is shown in Figs. 7, 8 and 9 for the three gas mixtures under study and for different levels of irradiation. The efficiency dependency on HV_{eff} has been interpolated by means of the Richards generalised logistic function [25]:

$$\epsilon = \frac{\epsilon_{max}}{\left[1 + \psi \cdot e^{-\beta(HV_{eff} - HV_0)}\right]^{1/\psi}} \qquad (2)$$

where ϵ_{max} represents the asymptotic efficiency; β describes the steepness of the curve; ψ ranges between 0 and 1 and parameterises the slower growth of the curve observed for eco-gas mixtures; HV_0 sets the displacement of the curve along the x-axis for fixed ψ and β.

---

[3] Hereafter, the gamma cluster rate values reported as reference at different levels of irradiation are efficiency corrected.

Fig. 6 Gamma cluster rate as a function of HV_{eff} for the thin-RPC operated with eco3 gas mixture. Results are shown for the vertical strip plane, at 6 m (top) and 3 m (bottom) from the source
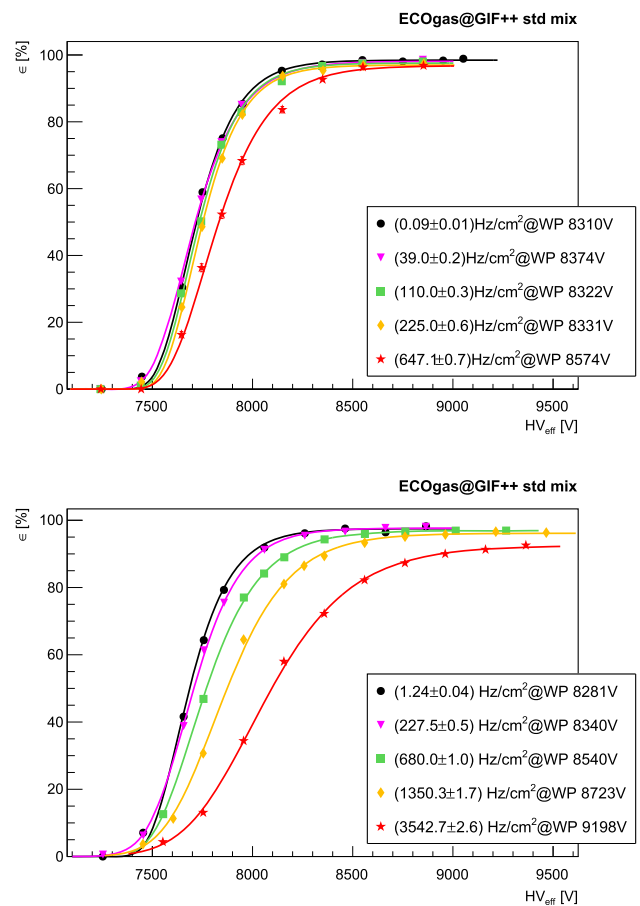

Fig. 7 Efficiency as a function of HV_{eff} for the standard gas mixture. Results are shown at 6 m (top) and 3 m (bottom) from the source and at different gamma cluster rates (efficiency corrected) evaluated at the detector WP

The detector working point is defined as the HV_{eff} value at which the 2D efficiency reaches 99% of the asymptotic value approached by the Richard function, therefore representing the optimal operational voltage at which the detector is fully efficient. For this reason, in the following the different levels of irradiation will be expressed in terms of the efficiency corrected gamma cluster rate measured by the detector at the WP.

The thin-RPC, operated with the standard gas mixture at the WP, shows an average 2D detection efficiency at source off of about 97%. When exposed to medium rates, up to about 1 kHz/cm^2, this value is reduced by about 1%. At higher particle rates, up to about 4 kHz/cm^2, an overall degradation at the level of about 6% is observed together with a progressive shift of the WP toward higher values (about 1 kV shift when the highest level of irradiation is applied).

When operated with eco2 gas mixture at WP and source off, the average 2D efficiency is about 96%. This value gradually decreases with increasing irradiation level, showing a maximum reduction of about 6% for medium rates and about 14% when the rate approaches 4 kHz/cm^2.

Similar results have been obtained for the thin-RPC flushed with the eco3 gas mixture at WP. Its average 2D efficiency is about 96% at source off and decreases to about 90% for particle rates of the order of 1 kHz/cm^2, reaching about 84% when exposed to the maximum level of irradiation. As for the standard mixture, a progressive shift of the WP toward higher values has been observed for increasing irradiation conditions with both eco-friendly alternatives. The maximum increase amounts to about 1.5 kV.

4.3 Cluster size

A set of adjacent strips is considered a *cluster* if they are fired within a certain time, hereafter referred to as *clustering time*. The clustering time has been evaluated to be 14 ns at the efficiency plateau and source off for the standard gas mixture.

The average muon cluster size as a function of the relative difference between the HV_{eff} and the detector WP (ΔV_{WP}) at different gamma cluster rates, is shown in Figs. 10, 11 and 12 for the three gas mixtures.
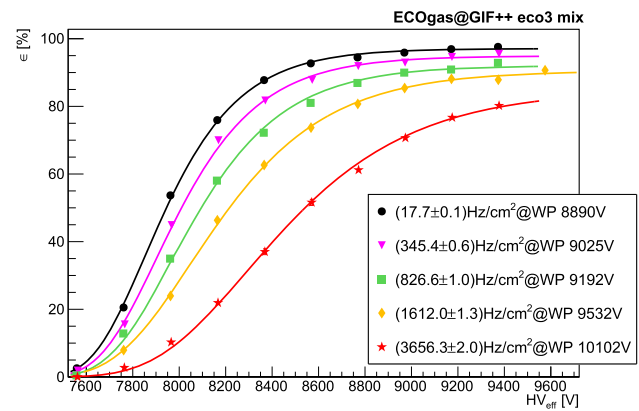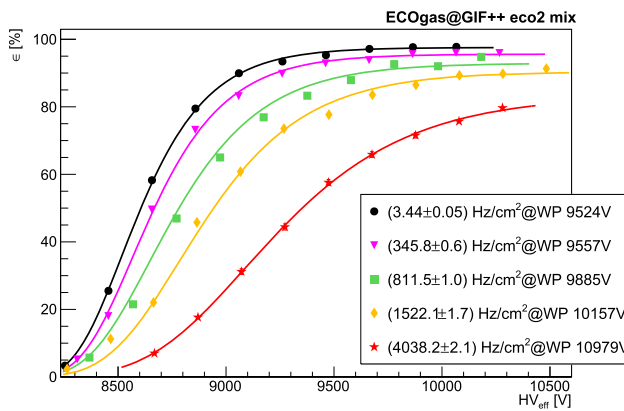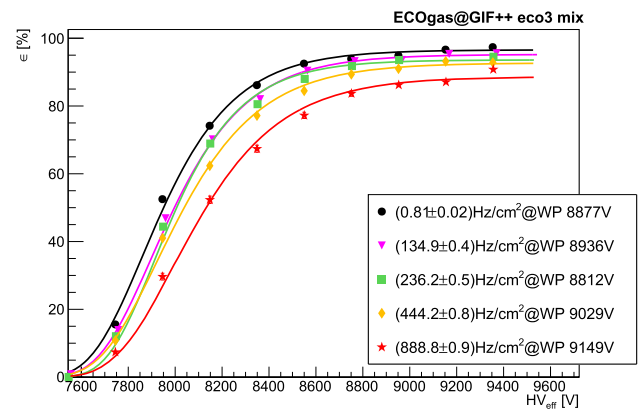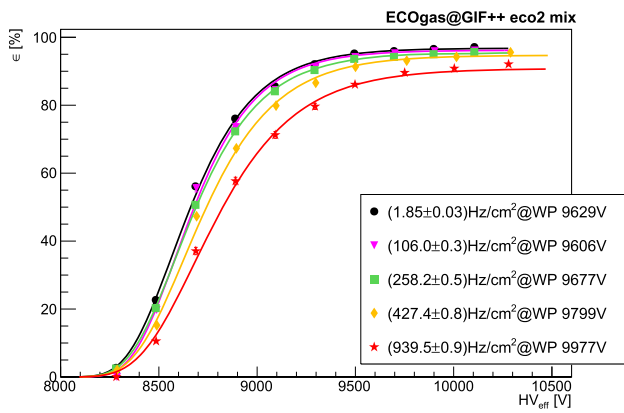
Fig. 8 Efficiency as a function of HV_{eff} for the eco2 gas mixture. Results are shown at 6 m (top) and 3 m (bottom) from the source and at different gamma cluster rates (efficiency corrected) evaluated at the detector WP

Fig. 9 Efficiency as a function of HV_{eff} for the eco3 gas mixture. Results are shown at 6 m (top) and 3 m (bottom) from the source and at different gamma cluster rates (efficiency corrected) evaluated at the detector WP

All the distributions show an average cluster size which slightly increases with HV_{eff}, while it decreases with increasing irradiation at fixed ΔV_{WP}. This effect is more pronounced for the eco-friendly gas mixtures. At the WP and fixed gamma cluster rate, the average muon cluster sizes for the standard, eco2 and eco3 gas mixtures are generally consistent within 10%, with typical values about 2.2. A similar behaviour has been observed for the average gamma cluster size, with typical values of about 2.1 at WP for the three mixtures.

Figures 13 and 14 show the fraction of events with an average muon cluster size greater than 4, $F(C_s > 4)$, when the RPC is 3 m far from the source. This is a key parameter for quantifying the number of events characterised by a charge content larger than that corresponding to avalanches in the same mixture, thus indicating a transition from avalanche to streamer operation mode [21]. The larger this fraction, the worse the impact on the performance and longevity of the detector will be. At source off and at WP, $F(C_s > 4)$ shows a slight increase for the eco-friendly alternatives under study. Comparing eco3 to the standard gas mixture, the increase is about 3%. The effect is significant for $\Delta V_{WP} > 0$, while it appears to be mitigated as gamma irradiation increases.

4.4 Current

The current absorbed by the HV power supply channel connected to the RPC under test has been monitored every second, both during the in-spill and out-of-spill data acquisitions. As shown in Fig. 15, the current can vary considerably depending on whether it is registered during the beam spill or not.

The average value of the current and its associated error have been evaluated out-of-spill by means of a Gaussian fit around the peak (Fig. 15) and plotted as a function of the relative difference between the HV_{eff} and the detector WP for the three gas mixtures, at different levels of irradiation, in Figs. 16, 17 and 18.

As expected, an overall increasing trend of the average current with HV_{eff} and with the irradiation rate is observed independently of the gas mixture in use. In case of eco-mixtures, current values are generally higher with respect to what measured with the standard one. At the WP and at the maximum irradiation rate, this increasing factor is about 2 for both eco2 and eco3 at 6 m from the source. At 3 m, a current of about 700 μA was measured when the RPC was operated at the
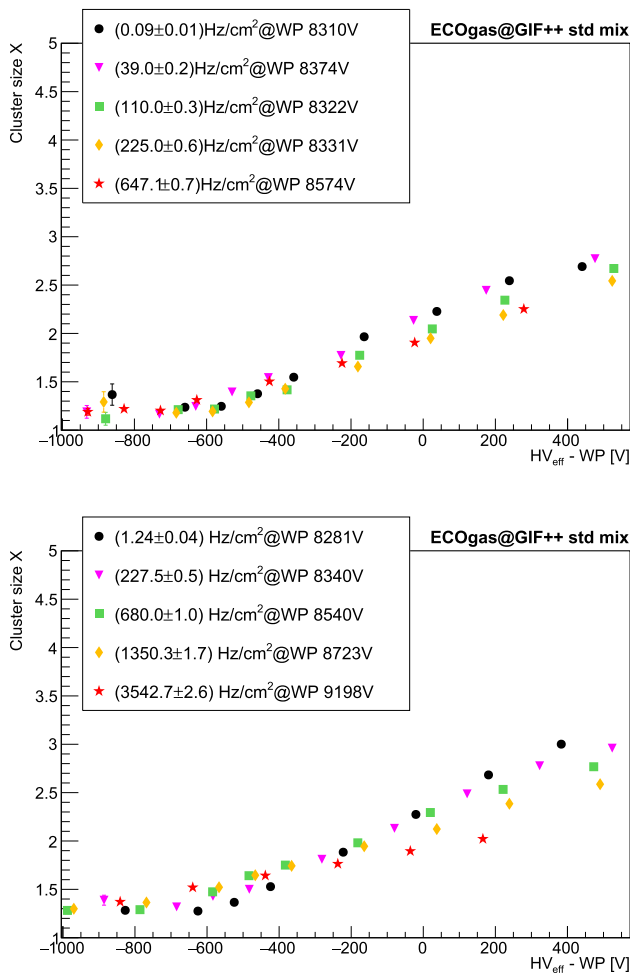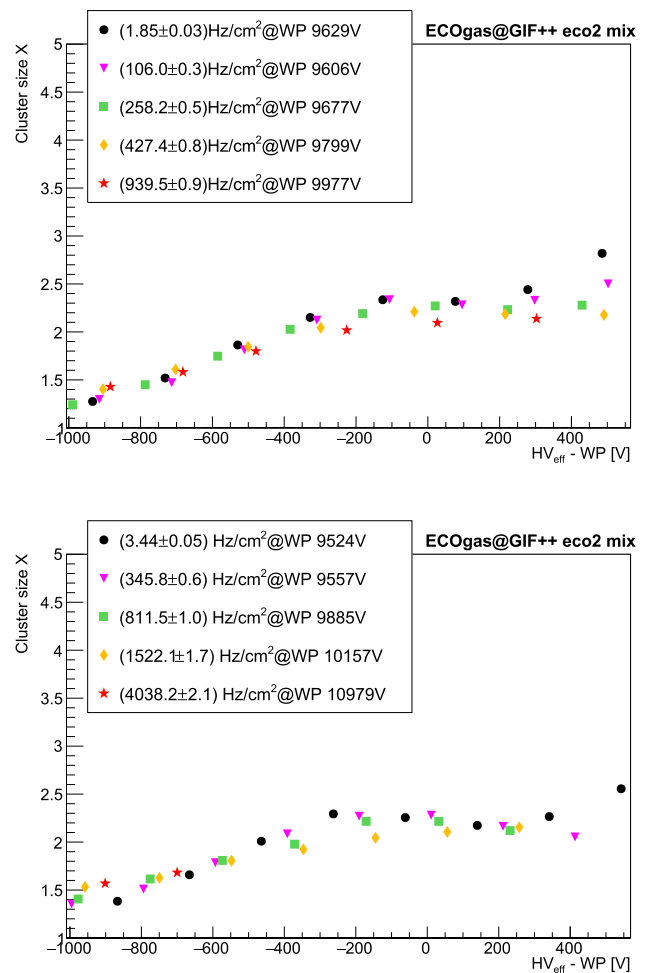
Fig. 10 Average muon cluster size as a function of the relative difference between the HV_{eff} and the detector WP for the standard gas mixture. Results are shown for the vertical strip plane, at 6 m (top) and 3 m (bottom) from the source and at different gamma cluster rates (efficiency corrected) evaluated at the detector WP

Fig. 11 Average muon cluster size as a function of the relative difference between the HV_{eff} and the detector WP for the eco2 gas mixture. Results are shown for the vertical strip plane, at 6 m (top) and 3 m (bottom) from the source and at different gamma cluster rates (efficiency corrected) evaluated at the detector WP

WP and at the maximum irradiation rate with the standard mixture. For the eco-friendly ones values even higher than 1 mA, which is the current limit for the power supply in use, would be reached. The expected values, based on the extrapolation of measured data, are about 1.3 mA for eco2 and about 1.2 mA for eco3 mixture, about two times higher with respect to the standard one in the same working conditions.

5 Conclusions

The performance of a thin single-gap RPC operated with HFO/CO_2-based gas mixtures and exposed at particle rates up to several kHz/cm^2 has been studied and compared to the standard one.

The results demonstrate that, at a fixed level of irradiation, both the eco-friendly gas mixtures show higher WP values with respect to the standard one. For particle rates increasing from source off up to about 1 kHz/cm^2, the detector operated with the three gas mixtures shows similar performances in terms of 2D detection efficiency, while higher absorbed currents (a factor of about 2) are registered for both eco2 and eco3. At higher rates, of the order of 4 kHz/cm^2, the eco-friendly mixtures seem to be less performing, showing a much slower growth of the 2D efficiency curve due to very high absorbed currents (about 1 mA) and a lower overall efficiency, estimated to be of about 84% at the WP. Moreover, the fraction of events characterised by a large charge content, indicating a transition of the detector from the avalanche to the streamer operation mode, is more pronounced for the eco-friendly mixtures, in particular for eco3 where the CO_2/HFO ratio is higher.
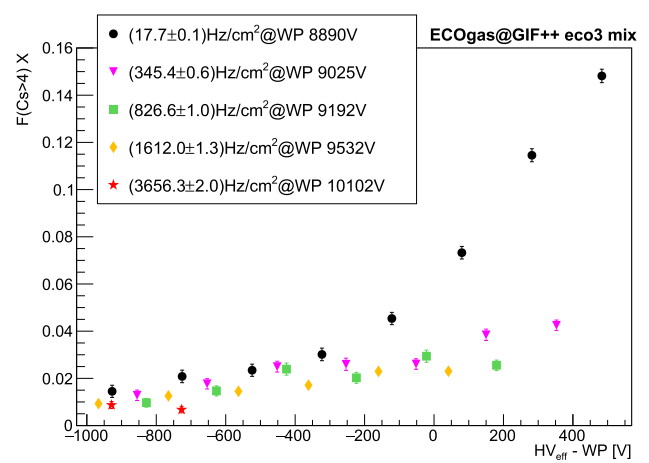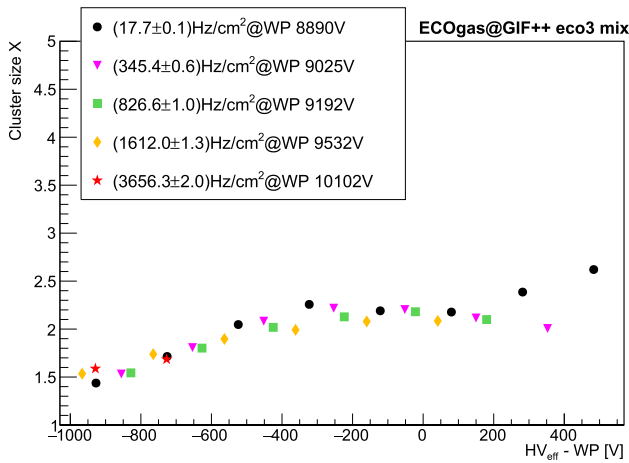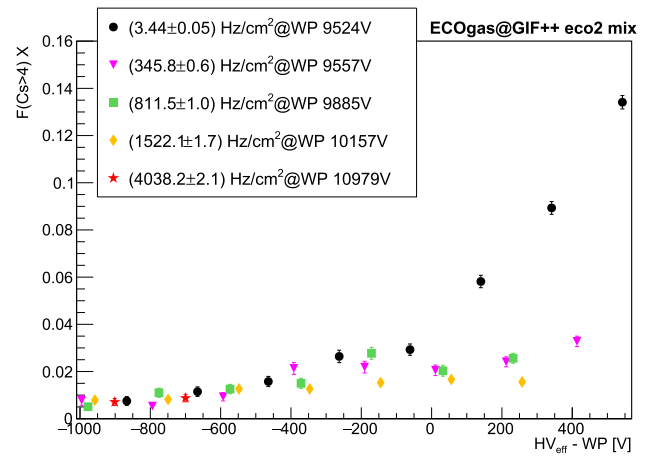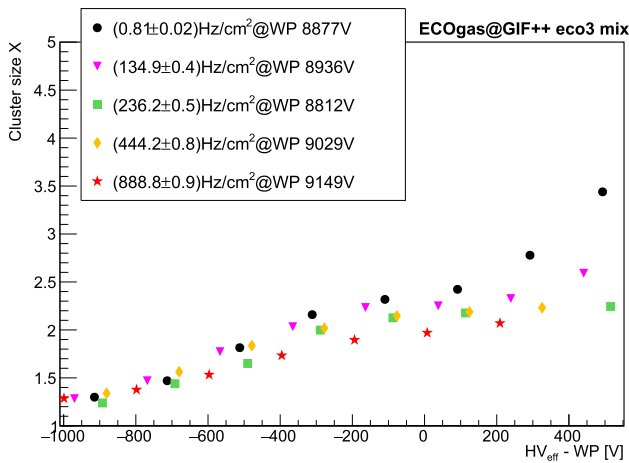
Fig. 12 Average muon cluster size as a function of the relative difference between the HV_{eff} and the detector WP for the eco3 gas mixture. Results are shown for the vertical strip plane, at 6 m (top) and 3 m (bottom) from the source and at different gamma cluster rates (efficiency corrected) evaluated at the detector WP
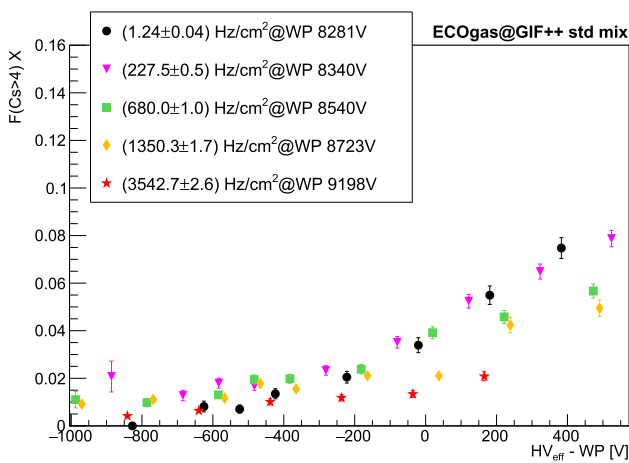
Fig. 14 Fraction of events with a cluster size X greater than 4 as a function of the relative difference between the HV_{eff} and the detector WP, at 3 m from the source for the eco2 (top) and eco3 (bottom) gas mixtures

Fig. 13 Fraction of events with a cluster size X greater than 4 as a function of the relative difference between the HV_{eff} and the detector WP, at 3 m from the source for the standard gas mixtures
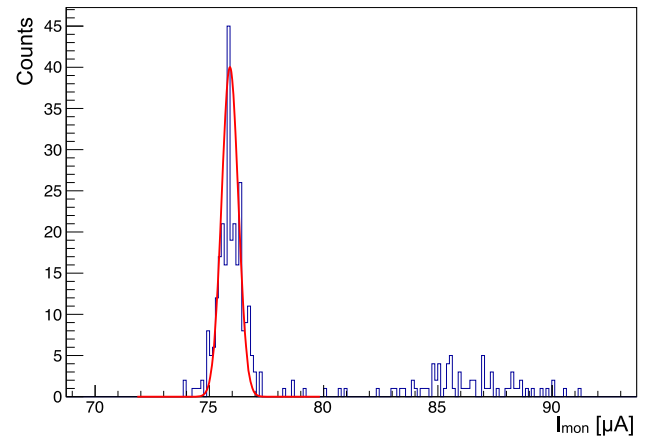
Fig. 15 Typical distribution of the absorbed current in presence of muon beam and gamma source. Lower values (peak at left) correspond to the presence of gamma irradiation only (out-of-spill condition). Highest values (bump at right) correspond to the presence of both beam spill and gamma irradiation (in-spill)
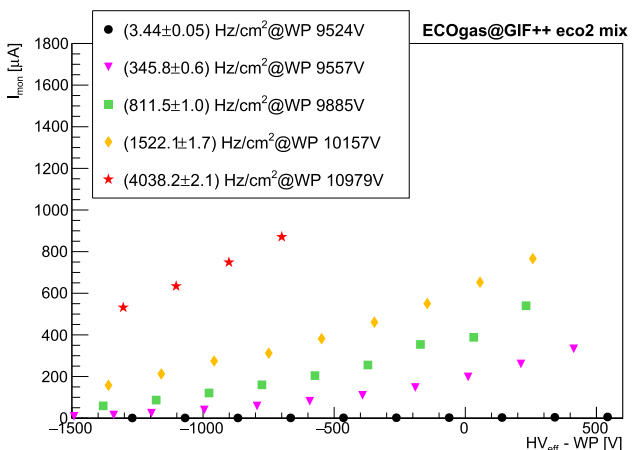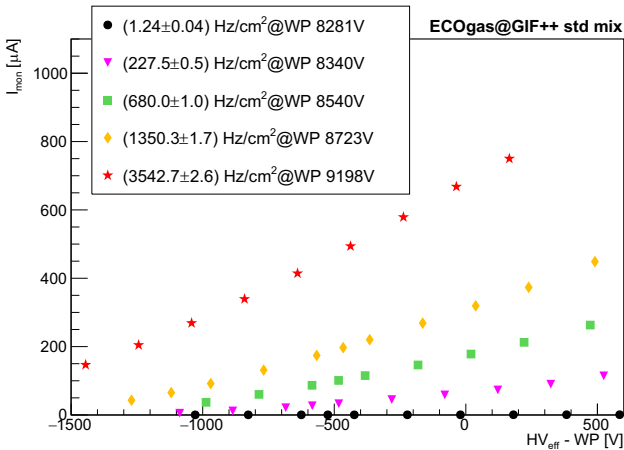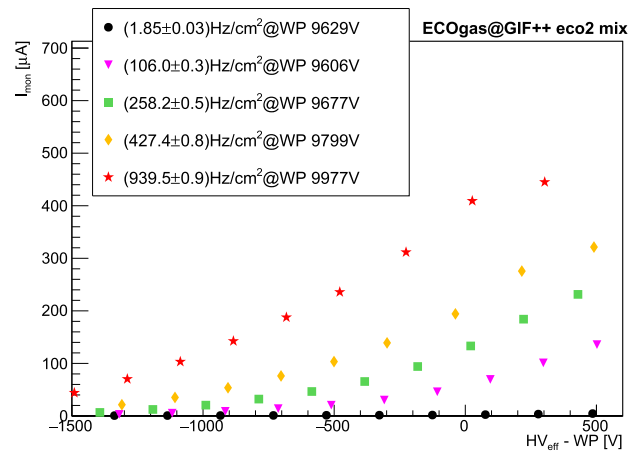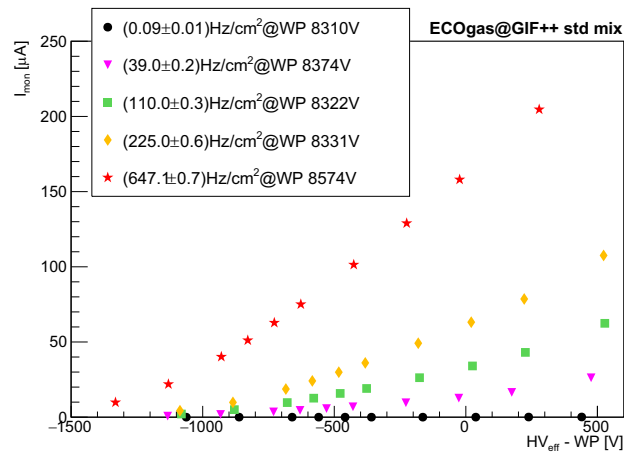
Fig. 16 Current as a function of the relative difference between the HV_{eff} and the detector WP, for the standard gas mixture. Results are shown at 6 m (top) and 3 m (bottom) from the source and at different gamma cluster rates (efficiency corrected) evaluated at the detector WP

Fig. 17 Current as a function of the relative difference between the HV_{eff} and the detector WP, for the eco2 gas mixture. Results are shown at 6 m (top) and 3 m (bottom) from the source and at different gamma cluster rates (efficiency corrected) evaluated at the detector WP

Based on these results, eco2 and eco3 gas mixtures could be good alternatives to the standard one in view of future HEP middle-high rate applications. However, an in-depth study on their effect on long-term performance is needed. For very high rate applications, their use requires additional steps forward in terms of new RPC layouts, materials and/or FE electronics, towards reduced <Q> and gas-gap thickness. The eco2 mixture has been selected for further tests currently ongoing at the GIF++, where also RPC detectors long-term performances will be carefully studied.
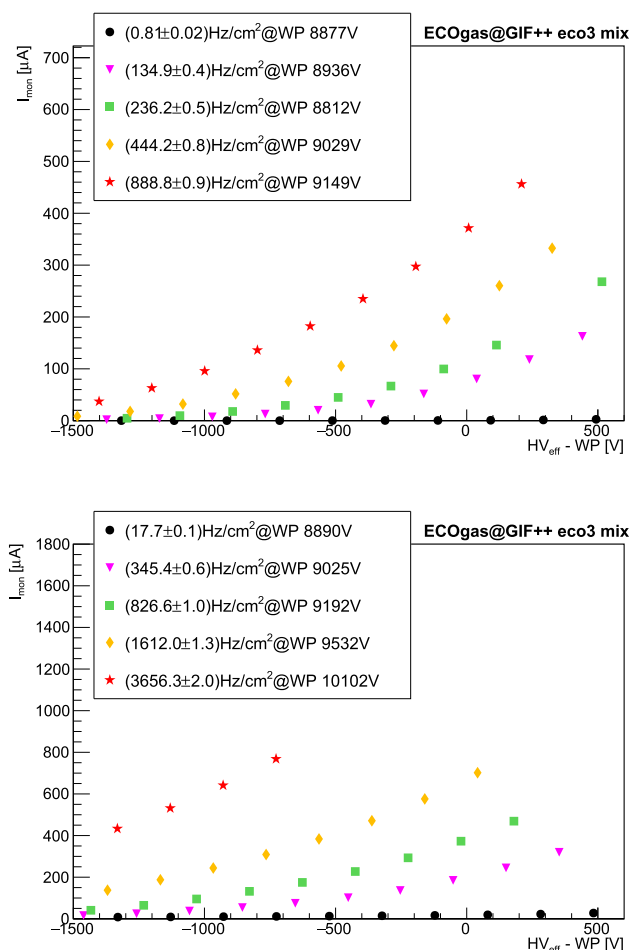
Fig. 18 Current as a function of the relative difference between the HV$_{eff}$ and the detector WP, for the eco3 gas mixture. Results are shown at 6 m (top) and 3 m (bottom) from the source and at different gamma cluster rates (efficiency corrected) evaluated at the detector WP

Data Availability Statement This manuscript has no associated data. [Authors' comment: The datasets used in the current study are available from the corresponding authors upon reasonable request.]

Code Availability Statement The manuscript has no associated code/software. [Author's comment: This manuscript has no associated code/software.]

References

1. R. Cardarelli, V. Makeev, R. Santonico, Avalanche and streamer mode operation of resistive plate chambers. Nucl. Instrum. Methods A **382**, 470–474 (1996). https://doi.org/10.1016/S0168-9002(96)00811-X
2. ECFA Detector R&D Roadmap Process Group, The 2021 ECFA detector research and development roadmap, CERN-ESU-017 (2020). https://doi.org/10.17181/CERN.XDPL.W2EX
3. The European Parliament and the Council of the European Union, Official Journal of the European Union, L 150, 20.5.2014, p.195-230. http://data.europa.eu/eli/reg/2014/517/oj (2014)
4. M. Capeans, I. Glushkov, R. Guida, F. Hahn, S. Haider, Optimization of a closed-loop gas system for the operation of resistive plate chambers at the Large Hadron Collider experiments. Nucl. Instrum. Methods A **661**, S214–S221 (2012). https://doi.org/10.1016/j.nima.2010.08.077
5. M. Capeans, R. Guida, B. Mandelli, Strategies for reducing the environmental impact of gaseous detector operation at the cern lhc experiments. Nucl. Instrum. Methods A **845**, 253–256 (2017). https://doi.org/10.1016/j.nima.2016.04.067
6. R. Guida, B. Mandelli, G. Rigoletti, Studies on alternative eco-friendly gas mixtures and development of gas recuperation plant for RPC detectors. Nucl. Instrum. Methods A **1039**, 167045 (2022). https://doi.org/10.1016/j.nima.2022.167045
7. M. Corbetta, R. Guida, B. Mandelli, G. Rigoletti, Gas R&D on gas recirculation and recuperation for the Resistive Plate Chamber detectors. JINST **15**(10), C10028 (2020). https://doi.org/10.1088/1748-0221/15/10/C10028
8. D. Pfeiffer et al., The radiation field in the gamma irradiation facility gif++ at cern. Nucl. Instrum. Methods Phys. Res. Sect. A Accel. Spectrom. Detect. Assoc. Equip. **866**, 91–103 (2017). https://doi.org/10.1016/j.nima.2017.05.045
9. M. Abbrescia, V. Peskov, P. Fonte, Resistive Gaseous Detectors: Designs, Performance, Perspectives, Wiley-VCH. Verlag GmbH & Co. KGaA (2018). https://doi.org/10.1002/9783527698691
10. R.L. Workman, Others, Review of Particle Physics, PTEP 2022 (2022) 083C01. https://doi.org/10.1093/ptep/ptac097
11. T. Dai et al., Low resistance bakelite rpc study for high rate working capability. J. Instrum. **9**, C11013 (2014). https://doi.org/10.1088/1748-0221/9/11/C11013
12. M. Abbrescia, Improving rate capability of resistive plate chambers. J. Instrum. **11**(10), C10001 (2016). https://doi.org/10.1088/1748-0221/11/10/C10001
13. G. Aielli et al., Improving the rpc rate capability. J. Instrum. **11**, P07014 (2016). https://doi.org/10.1088/1748-0221/11/07/P07014
14. K. Shchablo, I. Laktineh, M. Gouzevitch, C. Combaret, L. Mirabito, Performance of the cms rpc upgrade using 2d fast timing readout system. Nucl. Instrum. Methods Phys. Res. Sect. A Accel. Spectrom. Detect. Assoc. Equip. **958**, 162139 (2020). https://doi.org/10.1016/j.nima.2019.04.093
15. X. Fan, Precise measurement of gas parameters in a realistic RPC configuration: the currently used R134a gas and a potential alternative eco-gas. Nucl. Inst. Methods Phys. Res. A **1024**, 166124 (2022). https://doi.org/10.1016/j.nima.2021.166124
16. B. Liberti et al., Further gas mixtures with low environment impact. JINST **11**(09), C09012 (2016). https://doi.org/10.1088/1748-0221/11/09/C09012
17. CMS Collaboration, The Phase-2 Upgrade of the CMS Muon Detectors, CERN-LHCC-2017-012, CMS-TDR-016 (2017)

18. A. Bianchi et al., Characterization of tetrafluoropropene-based gas mixtures for the Resistive Plate Chambers of the ALICE muon spectrometer. JINST **14**, P11014 (2019). https://doi.org/10.1088/1748-0221/14/11/P11014

19. R. Guida, et al., Performance studies of RPC detectors with new environmentally friendly gas mixtures in presence of LHC-like radiation background. Nucl. Inst. Methods Phys. Res. A (958), 162073 (2020). https://doi.org/10.1016/j.nima.2019.04.027

20. R. Albanese et al., RPC-based muon identification system for the neutrino detector of the SHiP experiment. JINST **18**(02), P02022 (2023). https://doi.org/10.1088/1748-0221/18/02/P02022

21. M. Abbrescia, et al., High-rate tests on Resistive Plate Chambers operated with eco-friendly gas mixtures. Eur. Phys. J. C **84**, 300 (2024). https://doi.org/10.1140/epjc/s10052-024-12545-8

22. L. Quaglia, D. Ramos, et al., Preliminary results on the long term operation of rpcs with eco-friendly gas mixtures under irradiation at the cern gamma irradiation facility, Submitted to Eur. Phys. J. Plus (2023). arXiv:2311.17574

23. P. Dupieux, B. Joly, F. Jouve, S. Manen, R. Vandaële, Upgrade of the ALICE muon trigger electronics. J. Instrum. **9**(09), C09013–C09013 (2014). https://doi.org/10.1088/1748-0221/9/09/c09013

24. The H4 Secondary Beam Line of EHN1/SPS. https://sba.web.cern.ch/sba/BeamsAndAreas/H4/H4_presentation.html

25. F. J. Richards, A flexible growth function for empirical use. J. Exp. Bot. **10**(2), 290–301 (1959). https://doi.org/10.1093/jxb/10.2.290